Architectures of Polyacrylic Acid

Subjects: Nanoscience & Nanotechnology

Contributor: Mahmood Barani , hassan arkaban , , Narendra Pal Singh Chauhan , Sapana Jadoun , Payam Zarrintaj

Polyacrylic acid (PAA) is a non-toxic, biocompatible, and biodegradable polymer that gained lots of interest in recent years. PAA nano-derivatives can be obtained by chemical modification of carboxyl groups with superior chemical properties in comparison to unmodified PAA.

polyacrylic acid (PAA) synthesize polymerizations

1. Nanofibers

Nanofibers (NFs) have gained a particular interest owing to their unique physical and structural properties, i.e., large surface area, increased porosity, small pore size and fiber diameter, increased flexibility during functionalization of the surface [1]. Additionally, these possess high liquid or air permeability and rapid internal surfaces and form strong hydrogen bonds. Garza et al. [2] fabricated the nanofibers of PAA by subjecting the solutions of PAA for centrifugal spinning with various concentrations (9 to 14%) and speeds (4000 to 8000× *g* rpm), revealing different architectures of PAA nanofibers. When centrifuged at 6000× *g* rpm with 12 wt %. The average diameter of nanofibers was found 1100 nm when 12 wt % of PAA solution was placed for centrifugally spun at 6000× *g* rpm while the size was decreased to 900 nm in the case of 8000 rpm with the same concentration suggested the evaporation of the solvent in the fast spin rate resulting stretching of the nanofibers. The smallest diameter was found in the case of 9 wt %, which suggested that lower concentration led to smaller fiber average diameter, **Figure 1**a–c. PAA/PVA (in various molar ratios) electrospun nanofibers were stabilized by thermal crosslinking at 140 °C. The average diameter was found 309 ± 87 nm, 340 ± 83 nm, 290 ± 61 nm, and 221 ± 45 nm, for the molar ratios of 19.81, 35.65, 55.45 and 83.17, respectively for PAA/PVA [3]. This decrease resulted from the increment of conductivity and decrement of viscosity with increasing the PAA ratio. Eventually, the membranes maintained their fiber-based morphology joining at their points of contact after water immersion unveiled the porous architecture of PAA [4].

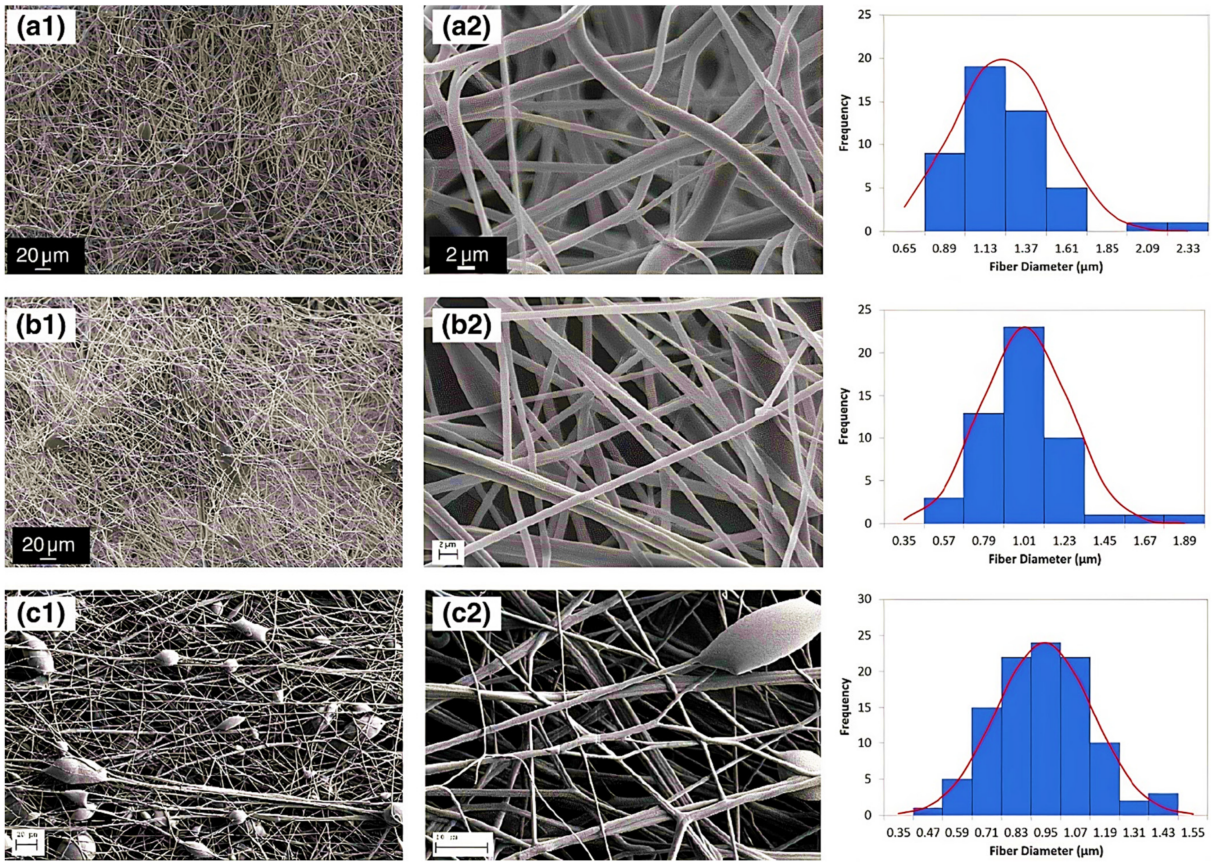

Figure 1. Diameter distribution and SEM micrographs of nanofibers of PAA (**a**) concentration of 12 wt% PAA and speed of 6000 rpm, (**b**) concentration of 12 wt% PAA concentration and speed of 8000 rpm, and (**c**) concentration of 9 wt% PAA concentration and speed of 4000 rpm. The SEM micrographs were taken at various magnifications: (**a1**,**b1**) 600×, (**c1**) 300×, (**a2**,**b2**) 7000×, and (**c2**) 15,000×. (Reprinted from Ref. [2] with permission).

2. Nanoparticles

Nanoparticles are materials with overall dimensions in the nanoscale, ie, under 200 nm. In recent years, these materials have emerged as important players in modern medicine, with clinical applications ranging from contrast agents in imaging to carriers for drug and gene delivery into tumors [5]. Nanoparticles of PAA have been extensively studied in biomedical applications such as drug delivery due to the unique capability to deliver drugs, genes, and proteins via the peroral route. The thiolated PAA nanoparticles were developed by Greindl et al. [6], whose architecture was covalently crosslinked via disulfide bonds. The cross-linkage of PAA with 2,2′-(ethylenedioxy)bis(ethylamine) (EDBEA) showed spherical morphology and 20–80 nm-sized nanoparticles [7], while the PAA-PS-Ag composite nanoparticles revealed spherical morphology with 3 ± 1.2 nm sized particles [8]. The exact morphology was obtained by Müller et al. [9] with a mean diameter <200 nm. The human fibrinogen binding kinetics depended on the size of negatively charged PAA/Au nanoparticles. The larger nanoparticles revealed binding with fibrinogen with a slower dissociation rate and increasing affinity. When the size of nanoparticles was 7 nm, the two nanoparticles were accommodated by each fibrinogen molecule, but when the size increased up to 10 nm, only one was adapted. The size increments up to 10–12 nm changes from one site to the two-site binding. The

bound nanoparticles felt more coulombic repulsion when the diameter was increased. Due to the flexibility of both binding sites, one nanoparticle with a sufficient diameter (15–17 nm) was also found enough for the interaction of fibrinogen. Hence, more than 12 nm, multiple protein molecules were found, **Figure 2**i [10]. PAA-coated iron oxide nanoparticles showed two types of molar mass (1800 and 5000) due to the different architecture of PAA chains, which influenced the molar mass. The magnetic diameter of these nanoparticles was found in between 7.3 to 11.9 nm [11]. The architecture of nanoparticles of PAA-chitosan (CS) was dependent on the synthesis and pH of the synthetic medium. The nanoparticles at 4.5 pH (acetic buffer solution) revealed consistent and solid spherical particles unveiling PAA-CS nanoparticles' matrix structure. PH 7.4 showed a dense core bounded by a fuzzy and diffuse coating 4 (ii). This architecture was due to ionic interaction between negatively charged PAA and positively charged CS. The different preparation processes of PAA-CS nanoparticles influenced the architecture of nanoparticles. When PAA was dropped into a solution of CS, the generation of PAA core occurred, and a membrane was formed on the PAA core surface resulting in a dark shell and soft-core spherical nanoparticles. On the other hand, When the CS solution was dropped in the PAA solution, the core of CS and membrane of PAA-CS were formed. There were no cavities formed in PAA-CS because of the not swelling of CS in acidic medium, **Figure 2**iii. These all structures were created due to the construction of samples, conditions of staining, etc. [12]. The PAA magnetic nanoparticles possessed uniform particles morphology with a 9.2 ± 2.6 nm average diameter while a hydrodynamic diameter of 246 ± 11 nm (n = 3) was measured by the dynamic light scattering (DLS) measurements [13]. The other magnetic nanoparticles of PAA had a 10 nm size and were semispherical in shape [14]. PAA-coated iron oxide nanoparticles revealed a 10.1 ± 2.4 nm mean particle size. These were stable in water, and variation in pH or enhancement in ionic strength resulted in aggregation of these nanoparticles in water [15].

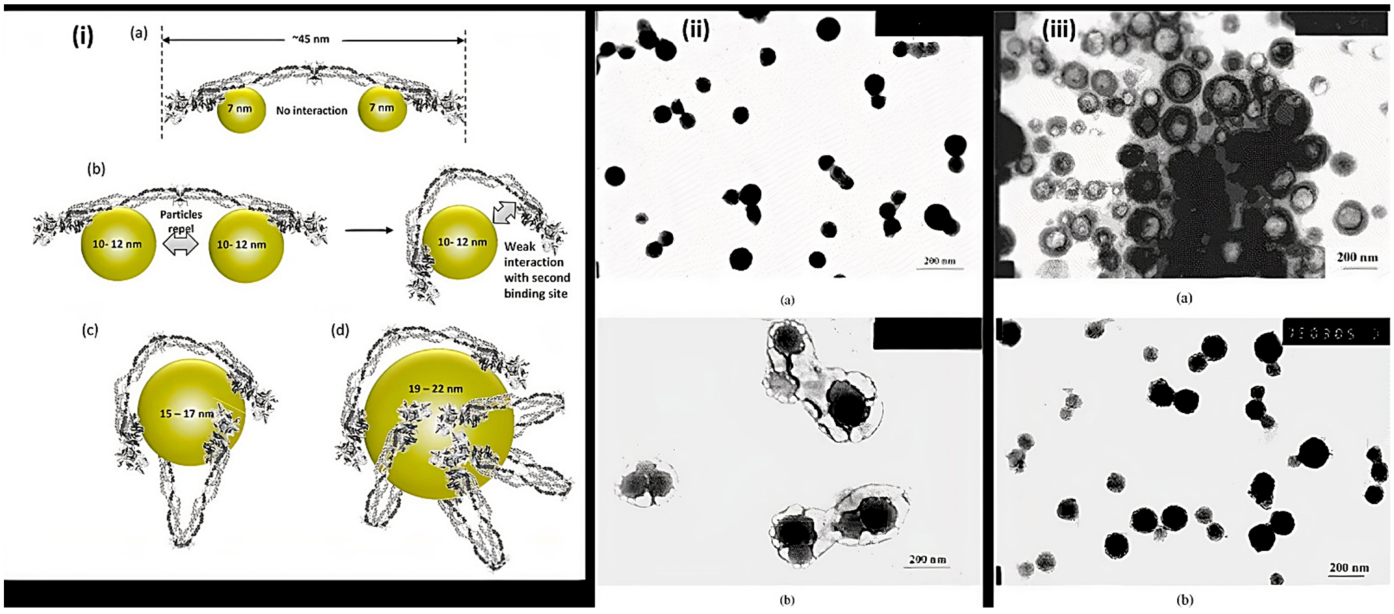

Figure 2. Representation of (**i**) binding of fibrinogen with PAA/Au nanoparticles (**a**) Binding of 7 nm nanoparticle to fibrinogen revealing each protein molecule accommodated two nanoparticles (**b**) 10–12 nm-sized nanoparticles prevent the binding of two particles to each fibrinogen due to the flexibility of fibrinogen at E domain of protein resulting the contact of second binding site with the nanoparticle (**c**,**d**) Larger nanoparticles (15–22 nm) can accommodate multiple fibrinogen molecules due to the larger surface area (**ii**) TEM of PAA-CS nanoparticles at (**a**)

pH = 4.5 and (**b**) at pH = 7.4. (**iii**) Morphology of PAA-CS nanoparticles synthesized by the various processes at 4.5: (**a**) CS dropping into PAA solution; (**b**) PAA dropping into CS solution, (Reprinted from Refs. [10][12] with permission).

3. Nanocapsules

Nanocapsules have been the most extensively studied for functional compounds delivery [16]. Nanocapsule possesses a large inner cavity which helps in the high loading of drugs and sustained release of drugs due to its capsule-like structure [17]. The hollow tailor-made 100 nm nanocapsules of PAA/CS were fabricated for antibiotic therapy by Belbekhouche et al. [18]. Nanocapsules of PAA-N-isopropylacrylamide (PNIPAm) hydrogel are presented in **Figure 3**i suggests the polymerization and crosslinking of PAA with PNIPAm to form the nanocapsule architecture and unveiled the round shape morphology (135 nm) for PAA-hydroxypropylcellulose (HPC) template particles. At the same time, the figure was seen in the 1st step above. After crosslinking with PNIPAm, the core (dark) shell (dusky) structure was seen, increasing the size to 230 nm. Even after removing the template, the particles maintained the spherical morphology with a larger inner cavity and thin shell having 50 ± 12.5 nm thickness, **Figure 3**ii [19]. The Nanosphere of PAA/BSA showed the 80 nm diameter while the nanocapsules revealed the 300–500 nm. These were synthesized using in situ polymerization, swelling, and re-aggregation. The interior diameter was found 100–200 nm, and glutaraldehyde (GA) cross-linked PAA/BSA nanospheres increased the stability. After absorbing the water molecules into PAA/BSA/GA also, nanocapsules were also formed. Microspheres presented the porous shape, and the hollows were small in nanocapsules that suggested that the architecture of PAA/BSA was fixed by cross-linking agents and reduced its flexibility, **Figure 3**iii [20]. Nanocapsules of PAA-*b*-PAN di-blocks were prepared using PAA macroinitiators using RAFT polymerization. The same architecture revealed monodisperse and spherical with 30~35 nm hydrodynamic diameter analyzed by dynamic light scattering and TEM. The aggregation of these nanocapsules was occurred by π-π interaction of the graphite layers [21]. In situ acrylic acid polymerization was done to obtain liposome nanocapsules coated with PAA with a mean diameter of 123 ± 21 nm [22]. The core-shell structure for copolymers of PAA was seen in the nanocapsules of PAA with an average diameter of 70 nm and 10 nm of shell thickness [23].

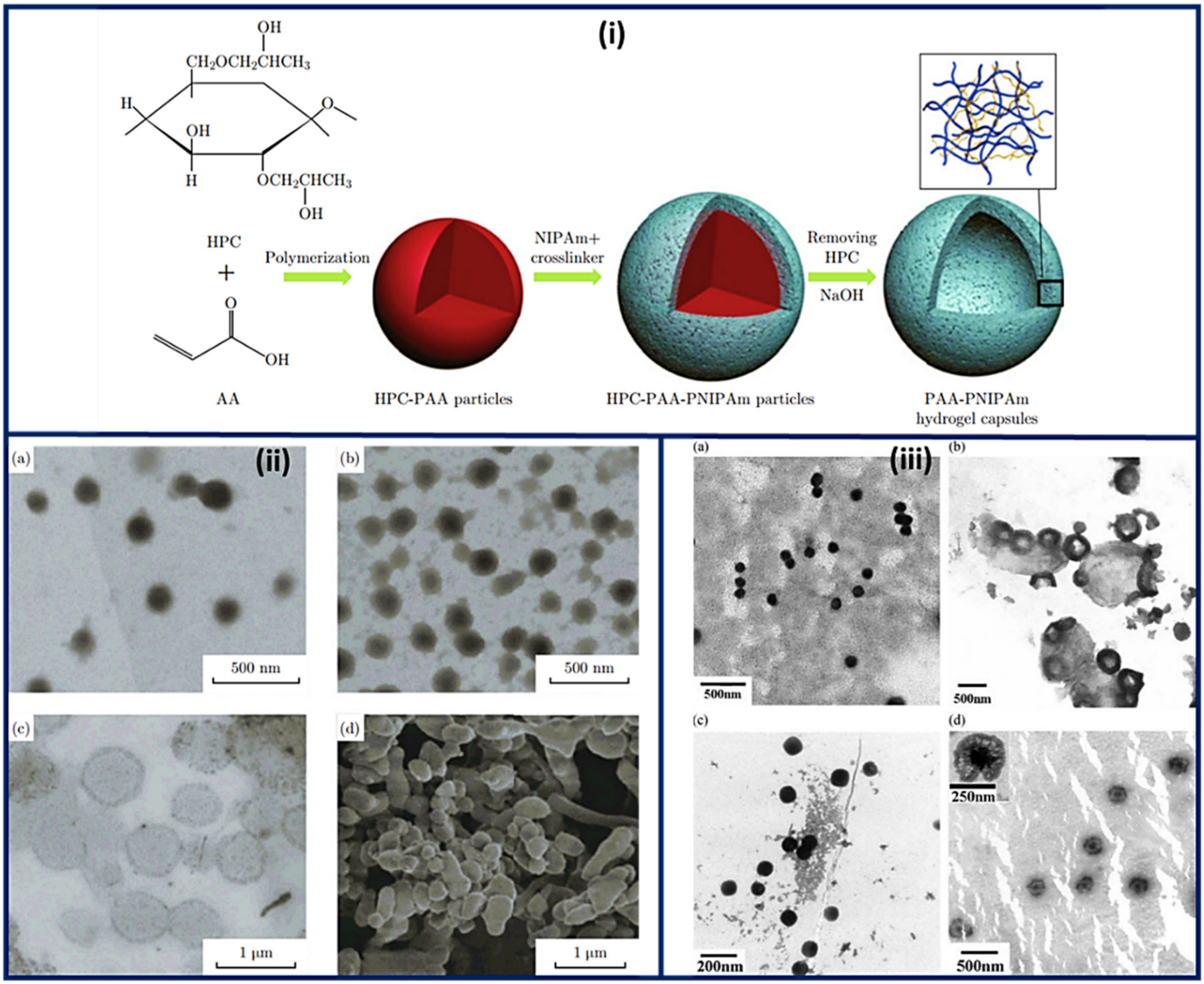

Figure 3. Schematic representation of the (**i**) synthesis and architecture of PNIPAm-PAA hydrogel capsules (**ii**) TEM micrographs of (**a**) PAA-HPC particles (pH 2.4) (**b**) PNIPAm-PAA-HPC composites (pH 2.4), (**c**) PNIPAm-PAA hydrogel capsules (pH 8.0) and (**d**) SEM image of PNIPAm-PAA hydrogel capsules after freeze-drying procedure. (**iii**) Morphology of nanosphere and nanocapsule of PAA/BSA (**a**) PAA/BSA, (**b**) nanocapsule of PAA/BSA, (**c**) PAA/BSA/GA, and (**d**) nanocapsule of PAA/BSA/GA. (Reprinted from Refs. [19][20] with permission).

4. Other Structures

Poly (acrylic acid-b-isoprene) cross-linked micelle structures were synthesized using calcium phosphate coating (20 nm thickness) having 60 ± 9 nm mean diameter, revealing the mineralization near or at surface regions of PAA. Additionally, nanocages were also formed. These hybrid materials were found stable for numerous months in water. Even though it aggregated and mineralized with time, there was no change seen in crystallization and diameter even after eight months (**Figure 4**a,b) [24]. Spherical microspheres of PAA/PVA of sequential interpenetrating network crosslinked with GA were obtained via SEM analysis. **Figure 4**c suggested spherical

morphology without any agglomerations. A smooth microspheres surface was obtained with no pores, and some particles were covered with polymeric debris, **Figure 4**d [25]

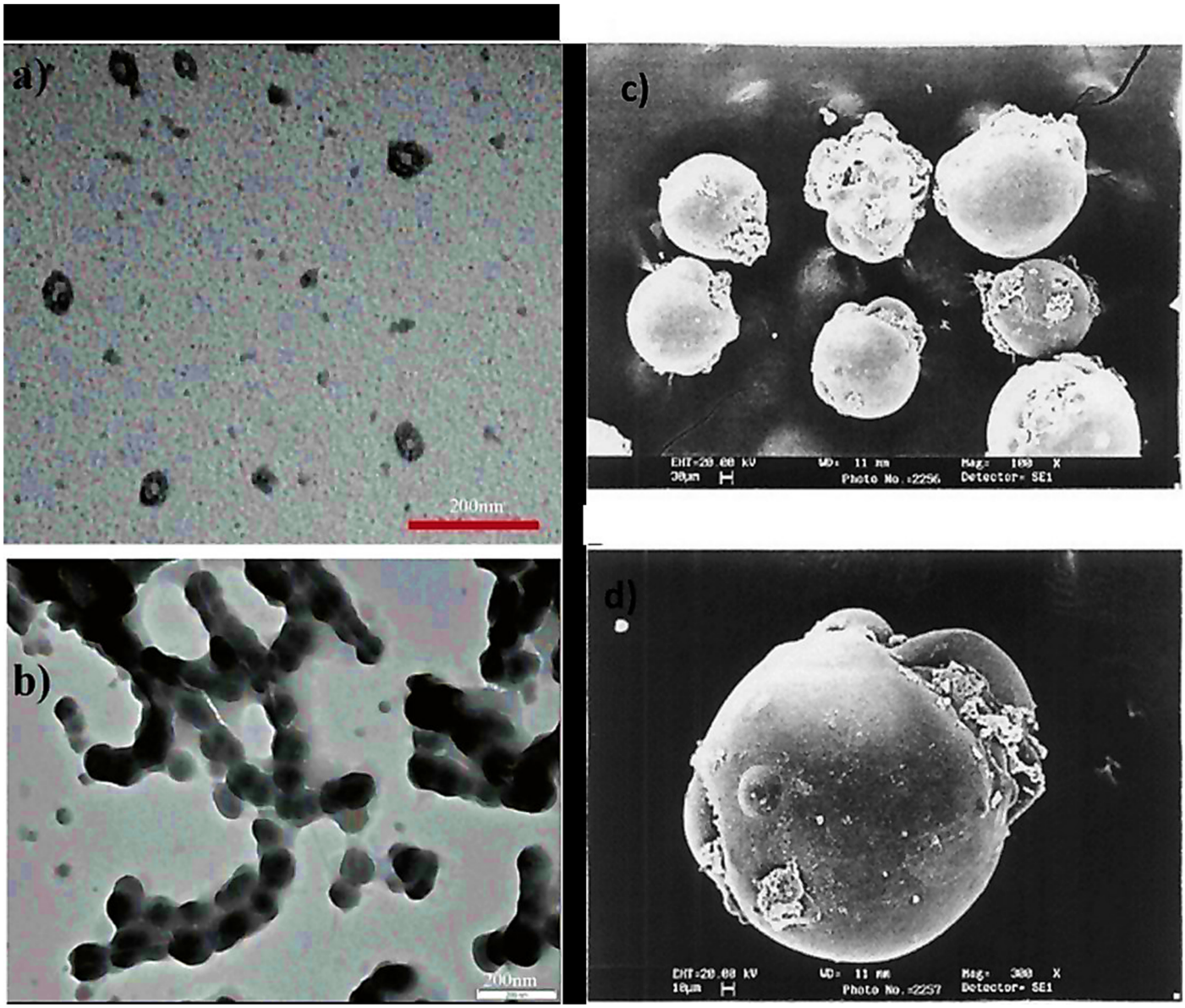

Figure 4. TEM micrographs of (**a**) cross-linked PAA-b-PI micelles covered with calcium phosphate, (**b**) PAA nanocages-Calcium phosphate displaying enhanced levels of aggregation and mineralization (after eight months) (**c**) SEM microspheres of PAA without forming agglomerations (spherical) (**d**) The smooth surface of microspheres without any pores. (Reprinted from Refs. [24][25] with permission).

References

1. Laraib, U.; Sargazi, S.; Rahdar, A.; Khatami, M.; Pandey, S. Nanotechnology-based approaches for effective detection of tumor markers: A comprehensive state-of-the-art review. Int. J. Biol. Macromol. 2021, 195, 356–383.

2. De la Garza, D.; De Santiago, F.; Materon, L.; Chipara, M.; Alcoutlabi, M. Fabrication and characterization of centrifugally spun poly (acrylic acid) nanofibers. J. Appl. Polym. Sci. 2019, 136, 47480.
3. Jin, X.; Hsieh, Y.-L. pH-responsive swelling behavior of poly (vinyl alcohol)/poly (acrylic acid) bi-component fibrous hydrogel membranes. Polymer 2005, 46, 5149–5160.
4. Santiago-Morales, J.; Amariei, G.; Letón, P.; Rosal, R. Antimicrobial activity of poly (vinyl alcohol)-poly (acrylic acid) electrospun nanofibers. Colloids Surf. B Biointerfaces 2016, 146, 144–151.
5. Duan, Z.; Yin, Q.; Li, C.; Dong, L.; Bai, X.; Zhang, Y.; Yang, M.; Jia, D.; Li, R.; Liu, Z. Milling force and surface morphology of 45 steel under different Al 2 O 3 nanofluid concentrations. Int. J. Adv. Manuf. Technol. 2020, 107, 1277–1296.
6. Greindl, M.; Bernkop-Schnürch, A. Development of a novel method for the preparation of thiolated polyacrylic acid nanoparticles. Pharm. Res. 2006, 23, 2183–2189.
7. Molnar, R.M.; Bodnar, M.; Hartmann, J.F.; Borbely, J. Preparation and characterization of poly (acrylic acid)-based nanoparticles. Colloid Polym. Sci. 2009, 287, 739–744.
8. Lu, Y.; Mei, Y.; Schrinner, M.; Ballauff, M.; Möller, M.W.; Breu, J. In situ formation of Ag nanoparticles in spherical polyacrylic acid brushes by UV irradiation. J. Phys. Chem. C 2007, 111, 7676–7681.
9. Müller, C.; Leithner, K.; Hauptstein, S.; Hintzen, F.; Salvenmoser, W.; Bernkop-Schnürch, A. Preparation and characterization of mucus-penetrating papain/poly (acrylic acid) nanoparticles for oral drug delivery applications. J. Nanopart. Res. 2013, 15, 1353.
10. Deng, Z.J.; Liang, M.; Toth, I.; Monteiro, M.J.; Minchin, R.F. Molecular interaction of poly (acrylic acid) gold nanoparticles with human fibrinogen. ACS Nano 2012, 6, 8962–8969.
11. Sanchez, L.M.; Martin, D.A.; Alvarez, V.A.; Gonzalez, J.S. Polyacrylic acid-coated iron oxide magnetic nanoparticles: The polymer molecular weight influence. Colloids Surf. A Physicochem. Eng. Asp. 2018, 543, 28–37.
12. Hu, Y.; Jiang, X.; Ding, Y.; Ge, H.; Yuan, Y.; Yang, C. Synthesis and characterization of chitosan–poly (acrylic acid) nanoparticles. Biomaterials 2002, 23, 3193–3201.
13. Ma, Y.-H.; Wu, S.-Y.; Wu, T.; Chang, Y.-J.; Hua, M.-Y.; Chen, J.-P. Magnetically targeted thrombolysis with recombinant tissue plasminogen activator bound to polyacrylic acid-coated nanoparticles. Biomaterials 2009, 30, 3343–3351.
14. Mahdavian, A.R.; Mirrahimi, M.A.-S. Efficient separation of heavy metal cations by anchoring polyacrylic acid on superparamagnetic magnetite nanoparticles through surface modification. Chem. Eng. J. 2010, 159, 264–271.

15. Couto, D.; Freitas, M.; Vilas-Boas, V.; Dias, I.; Porto, G.; Lopez-Quintela, M.A.; Rivas, J.; Freitas, P.; Carvalho, F.; Fernandes, E. Interaction of polyacrylic acid coated and non-coated iron oxide nanoparticles with human neutrophils. Toxicol. Lett. 2014, 225, 57–65.
16. Cerqueira, M.A.; Pinheiro, A.C.; Silva, H.D.; Ramos, P.E.; Azevedo, M.A.; Flores-López, M.L.; Rivera, M.C.; Bourbon, A.I.; Ramos, Ó.L.; Vicente, A.A. Design of bio-nanosystems for oral delivery of functional compounds. Food Eng. Rev. 2014, 6, 1–19.
17. Zhang, Y.; Hsu, B.Y.W.; Ren, C.; Li, X.; Wang, J. Silica-based nanocapsules: Synthesis, structure control and biomedical applications. Chem. Soc. Rev. 2015, 44, 315–335.
18. Belbekhouche, S.; Mansour, O.; Carbonnier, B. Promising sub-100 nm tailor made hollow chitosan/poly (acrylic acid) nanocapsules for antibiotic therapy. J. Colloid Interface Sci. 2018, 522, 183–190.
19. Nan, J.; Chen, Y.; Li, R.; Wang, J.; Liu, M.; Wang, C.; Chu, F. Polymeric hydrogel nanocapsules: A thermo and pH Dual-responsive carrier for sustained drug release. Nano-Micro Lett. 2014, 6, 200–208.
20. Wang, R.M.; Li, G.; Zhang, H.F.; He, Y.F.; He, N.P.; Lei, Z. Preparation of albumin—PAA nanocapsules and their controlled release behavior for drugs. Polym. Adv. Technol. 2010, 21, 685–690.
21. Aqil, A.; Detrembleur, C.; Gilbert, B.; Jérôme, R.; Jérôme, C. Controlled RAFT synthesis of polyacrylonitrile-b-poly (acrylic acid) diblocks as precursors of carbon nanocapsules with assistance of gold nanoparticles. Chem. Mater. 2007, 19, 2150–2154.
22. Scarioti, G.D.; Lubambo, A.; Feitosa, J.P.; Sierakowski, M.R.; Bresolin, T.M.; de Freitas, R.A. Nanocapsule of cationic liposomes obtained using “in situ” acrylic acid polymerization: Stability, surface charge and biocompatibility. Colloids Surf. B Biointerfaces 2011, 87, 267–272.
23. Zhang, W.-J.; Yan, Y.-Z.; Nagappan, S.; He, S.; Ha, C.-S.; Jin, Y.-S. Dual (thermo-/pH-) responsive P (NIPAM-co-AA-co-HEMA) nanocapsules for controlled release of 5-fluorouracil. J. Macromol. Sci. Part A 2021, 58, 860–871.
24. Perkin, K.K.; Turner, J.L.; Wooley, K.L.; Mann, S. Fabrication of hybrid nanocapsules by calcium phosphate mineralization of shell cross-linked polymer micelles and nanocages. Nano Lett. 2005, 5, 1457–1461.
25. Kurkuri, M.D.; Aminabhavi, T.M. Poly (vinyl alcohol) and poly (acrylic acid) sequential interpenetrating network pH-sensitive microspheres for the delivery of diclofenac sodium to the intestine. J. Control. Release 2004, 96, 9–20.